Effect of the Dielectric and Mechanical Properties of the Polymer Matrix on ZnO-Nanowire-Based Composite Nanogenerators Performance

Nicole Doumit, Guylaine Poulin-Vittrant

Effect of the Dielectric and Mechanical Properties of the Polymer Matrix on ZnO-Nanowire-Based Composite Nanogenerators Performance

Nicole DOUMIT, Guylaine POULIN-VITTRANT

GREMAN UMR 7347 CNRS, INSA Centre Val de Loire, Université de Tours, 3 rue de la chocolaterie, 41034 Blois, France.
E-mail: nicole.doumit@univ-tours.fr; guylaine.poulin-vittrant@univ-tours.fr

Keywords: Vertically Integrated Nanogenerator, ZnO nanowires, piezoelectricity, mechanical energy harvesting, Finite Element Model

Abstract

The effect of Young's Modulus and dielectric permittivity of the polymer matrix in vertically integrated nanogenerators (VING) on their output performance is studied by combining Finite Element Method (FEM) and analytical modeling. To conduct this study, an elementary cell is considered, based on one ZnO nanowire surrounded by the polymer matrix. We demonstrate that the polymer matrix should have the lowest Young's Modulus and permittivity as possible, in order to maximize the output voltage and power. Four different materials, which have already been proposed in literature for such composite VING, are then compared: Parylene C, PMMA, Al_2O_3 and PDMS. Simulation results show that PDMS, who has the lowest values of both Young's Modulus and permittivity, gives the highest output performance. Finally, the sensitivity to another design parameter – the surface density of nanowires – is calculated, and this study shows that choosing a polymer material with the lowest Young's Modulus and permittivity is more powerful to improve the VING performance.

1. Introduction

Over the past few years, piezoelectric nanowires (NWs) have attracted interest from researchers working on mechanical energy harvesting for autonomous sensors whose market is expected to grow, with the development of the Internet of Things.[1-3] As electroactive material within nanogenerators (NG), the piezoelectric and semiconducting NWs (usually ZnO or GaN) convert mechanical energy into electricity when strained by an external force.[4-7] The first NG proof of concept was presented in 2006,[8] with an experiment carried out with an AFM tip sweeping across a ZnO NWs array, leading to the generation of an electric voltage. In 2008, a single ZnO NW bonded horizontally on a flexible substrate was developed: [9] periodic bending of the substrate produced an alternative electric output from the NW. Since then, substantial progress has been made to integrate a large number of NWs together, aiming at harvesting electrical energy from all NWs simultaneously. The NG design has evolved with lateral, [9-11] radial [12,13] and vertical [11,14] NWs arrays. However, the Vertically Integrated NanoGenerator (VING) is the most used NG design because its fabrication and integration are often easier, especially when the synthesis

process leads to an array of NWs oriented orthogonally to the substrate. [5,15-17] Nanostructured materials like ZnO [5,17,18], GaN [19,20], PZT [21,22], $BaTiO_3$ [23,24], $NaNbO_3$ [25] and PVDF [26] have been used and studied as piezoelectric material within a VING. However, among them, ZnO is the most used material because it is lead free, biocompatible and it can be grown easily at low temperature (85°C) on several substrates [5,8,16,18], thanks to hydrothermal synthesis. Many filler materials with different properties (**Table 1**) have also been used (PMMA, Al_2O_3, PDMS, Parylene C…). [5,25,27] The performance of some VING devices using different types of materials is presented in **Table 2**. Hinchet *et al.* [15] have demonstrated that both the electrical potential and energy surface density could be improved by tuning the NW's density (represented by the ratio of NW diameter to the core cell width) to an optimum value, and by minimizing the thickness of the insulating layer. They also showed that PMMA was a good choice for the insulating material compared to other materials with higher Young's modulus. In another study, [5] they divided the insulating layer in two parts: the layer above NWs and the layer between NWs. They studied and compared the performance of NGs as a function of the top insulating layer material. Three type of material were chosen (SiO_2, Si_3N_4 and Al_2O_3), all of them presenting both a Young's modulus and dielectric permittivity higher than the interstitial insulator (PMMA). Authors proved that the usage of a high Young's modulus and permittivity for the top insulator maximizes the energy stored in the NG. However, none of the optimization research works investigated the best solution between optimizing the filler properties or optimizing the NWs' volume density (volume fraction of the piezoelectric material over the total volume of the composite layer) in order to obtain the highest generated voltage and/or power. Indeed, Young's modulus and dielectric permittivity values of the filler affect the VING performance since they influence the efficiency of the conversion of mechanical energy into electrical one. For this purpose, in this paper, the filler's Young's Modulus and permittivity were varied successively in order to obtain the most efficient VING, and this theoretical study was performed using HyMeSoVING method. [27] We show that the lower the filler's Young's modulus and permittivity, the higher the generated voltage and power. These results are compared to the increase in performance obtained when the NW's volume density is optimized.

Table 1: Young's modulus and relative dielectric permittivity of commonly used fillers

Filler material	**PDMS**	**Parylene C**	**PMMA**	**Al_2O_3**
Young's Modulus Y	360 - 870 kPa [28]	2.4 – 4 GPa [29]	2 – 4.5 GPa [30, 31]	345 – 409 GPa [32, 37]
Relative dielectric permittivity ϵ_{11}^F	2.5 – 3 [33]	2.7 – 6 [34]	2.85 – 3.6 [35, 36]	5.7 – 10 [37, 38, 39]

Table 2: State of the art on NGs performance

NW Material	Filler material	NW diameter	NW length	Number of NWs or NW's density	Applied force or pressure	Open-circuit voltage	Maximum power or power density	Reference
ZnO	PMMA	50 nm	600 nm	1	1 MPa (compression)	80 mV	-	[5]
ZnO	-	4 µm	200 µm	1	Bending of the substrate	50 mV	-	[9]
ZnO	PMMA	4 µm	400 nm	9	- (compression)	15 mV	2.8 nW/cm²	[40]
ZnO	Si_3N_4	~100 nm	5 nm	1	- (compression)	25 mV	-	[11]
ZnO	Parylene C	50 nm	0.5 µm	100 NW/µm²	13 N (compression)	9 V	-	[16]
GaN	HSQ	45 nm	1 µm	10^9 NWs/cm²	149 nN (compression)	350 mV	12.7 $mW.cm^{-3}$	[41]
ZnO + multiwall-carbon nanotubes	PDMS	30 nm	50 µm	-	Hammer knocking	7.5 V	18.75 µW	[42]
ZnO + multiwall-carbon nanotubes	PDMS	30 nm	50 µm	-	Foot stamp	30 V	-	[42]
ZnO	Al_2O_3	200 nm	3.5 µm	-	Bending	2.1 V	-	[43]

2. Theory

A VING can be described as a multi-layer device: First, the core of the structure consists on ZnO NWs array that converts mechanical energy into electrical energy via piezoelectric effect. Secondly, this NWs array is coated with an insulating layer which increases mechanical robustness and protects it from the electrical leakages and short circuits that could occur.[16] The third part is the top and bottom electrodes which are used to collect electrical charges. The principle of the mechanical energy harvesting with the VING device is the following: the applied mechanical forces compress the NWs along their z-axis. This compression generates a voltage difference across NWs due to the piezoelectric effect: negative charges appear at the top of the NWs and positive charges appear at the bottom electrode. The polarization-induced electric field drives a flow of electrons through the external circuit. A reverse flow of electrons occurs when the compression onto the VING decreases and the VING returns to the initial state.

HyMeSoVING (Hybrid Method for Simulation of VING) [27], a combination of a Finite Element (FE) model and an analytical model, is described in **Figure 1**: on one hand, the open-circuit voltage (V_{OC}) delivered by an elementary cell of the VING is calculated using FE analysis (here using COMSOL Multiphysics® software); on the other hand, the optimum resistive load (R_{opt}) of this elementary nanogenerator cell is estimated thanks to an equivalent electrical circuit

(**Figure 1**) whose parameters are homogenized ones, considering the active layer as a 1-3 piezocomposite. Using both results (V_{OC} and R_{opt}), the maximum average power delivered by the cell is then calculated. Finally, the performance of a full VING can then be deduced from the elementary cell's results by using the total number of NWs within the VING, as a scaling factor.

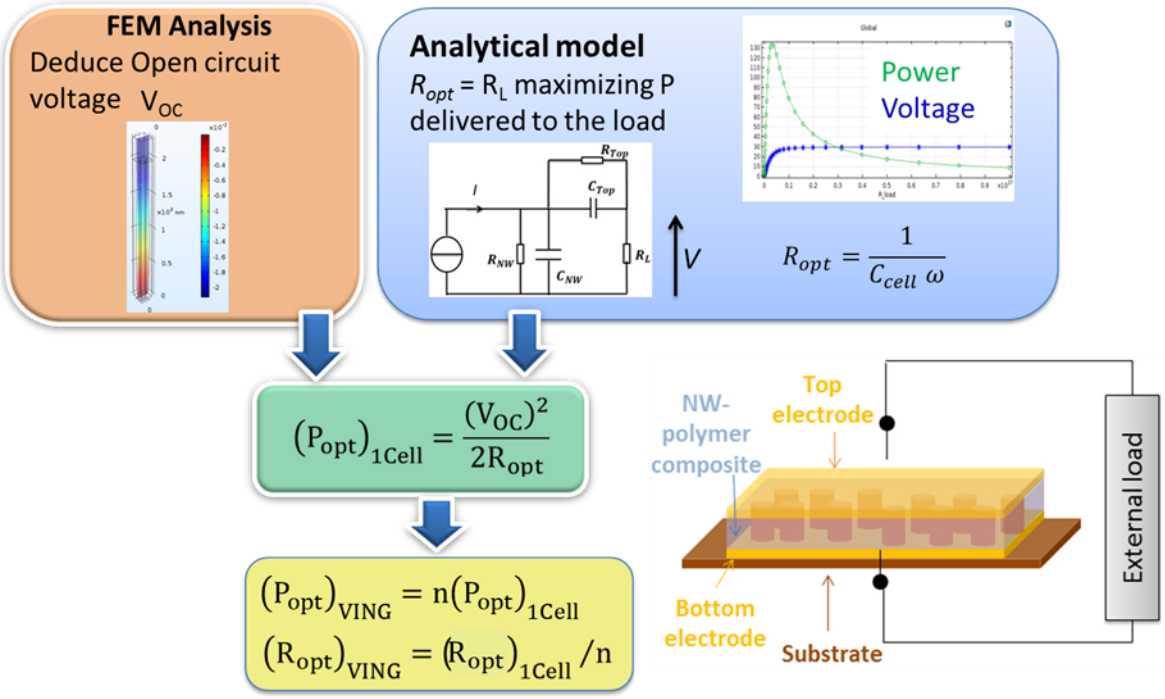

Figure 1: HyMeSoVING (Hybrid Method for Simulation of VING) schematic diagram.

Please note the elementary cell is composed of one ZnO NW (**Figure 2.a**) surrounded by the insulating matrix. Symmetry conditions are applied on the lateral edges, both in Solid Mechanics and Electrostatics modules used in COMSOL. In Solid Mechanics module, one symmetry condition is sufficient for all lateral edges, whereas in Electrostatics module two periodic conditions must be defined, one for x-axis edges and a second one for y-axis edges. The cell is clamped at the bottom face and a vertical surface force F is applied onto the top face.

The polymer matrix material is assumed to be purely elastic and dielectric. Therefore, its behavior is governed by Hooke's law and Poisson's equation:

$$\boldsymbol{T = cS} \tag{1}$$

$$\boldsymbol{\nabla . D = \rho_V} \tag{2}$$

where T is the stress tensor, S is the strain tensor, c is the stiffness tensor, D is the electrical displacement field and ρ_V is the volume charge density.

The NWs are considered as pure piezoelectric material. Therefore, electrical and mechanical laws are coupled, through the linear piezoelectric constitutive equations:

$$\boldsymbol{T} = \boldsymbol{c_E S} - \boldsymbol{e^t E} \tag{3}$$

$$\boldsymbol{D} = \boldsymbol{eS} - \boldsymbol{\epsilon E} \tag{4}$$

where c_E is the stiffness tensor for a constant electrical field $\boldsymbol{E}$, e is the piezoelectric coupling tensor in stress-charge notation and $\boldsymbol{\epsilon}$ is the electric permittivity tensor. The superscript t stands for the transpose of the matrix.

In the case of ZnO based devices, the piezocomposite can be described as a 1-3 composite (1D piezoelectric rods in a 3D insulating matrix). Smith and Auld [44] showed that the constitutive relations can be written as:

$$\overline{\boldsymbol{T_3}} = \bar{\boldsymbol{c}}_{\boldsymbol{33}}^{\boldsymbol{E}}\bar{\boldsymbol{S}}_{\boldsymbol{3}} - \bar{\boldsymbol{e}}_{\boldsymbol{33}}\bar{\boldsymbol{E}}_{\boldsymbol{3}} \tag{5}$$

$$\bar{\boldsymbol{D}}_{\boldsymbol{3}} = \bar{\boldsymbol{e}}_{\boldsymbol{33}}\bar{\boldsymbol{S}}_{\boldsymbol{3}} + \bar{\boldsymbol{\epsilon}}_{\boldsymbol{33}}^{\boldsymbol{S}}\bar{\boldsymbol{E}}_{\boldsymbol{3}} \tag{6}$$

where

$$\bar{c}_{33}^{E} = \delta\left(c_{33}^{E} - \frac{2(1-\delta)\left(c_{13}^{E}-c_{12}^{F}\right)^{2}}{\delta\left(c_{11}^{F}+c_{12}^{F}\right)+(1-\delta)\left(c_{11}^{E}+c_{12}^{E}\right)}\right) + (1-\delta)c_{11}^{F} \tag{7}$$

$$\bar{e}_{33} = \delta\left(e_{33} - \frac{2(1-\delta)e_{31}\left(c_{13}^{E}-c_{12}^{F}\right)}{\delta\left(c_{11}^{F}+c_{12}^{F}\right)+(1-\delta)\left(c_{11}^{E}+c_{12}^{E}\right)}\right) \tag{8}$$

$$\bar{\epsilon}_{33}^{S} = \delta\left(\epsilon_{33}^{S} + \frac{2(1-\delta)e_{31}^{2}}{\delta\left(c_{11}^{F}+c_{12}^{F}\right)+(1-\delta)\left(c_{11}^{E}+c_{12}^{E}\right)}\right) + (1-\delta)\epsilon_{11}^{F} \tag{9}$$

where superscript F stands for filler, superscript S stands for constant strain, superscript E stands for constant electric field and δ is the volume fraction of the piezoelectric material over the total volume of the composite layer, c_{11}^{F} and c_{12}^{F} are expressed using the constitutive equations for an isotropic material as follows: [45]

$$c_{11}^{F} = \frac{Y.(1-\eta)}{(1+\eta).(1-2\eta)} \tag{10}$$

$$c_{12}^{F} = \frac{Y.\eta}{(1+\eta).(1-2\eta)} \tag{11}$$

where Y represents the filler Young's Modulus and η its Poisson ratio.

Passive components of the equivalent electrical circuit are calculated using the following equations: [27]

$$C_{NW} = \frac{A\bar{\epsilon}_{33}^{S}}{L_{NW}} \quad (12)$$

$$C_{Top} = \frac{A\epsilon_{11}^{F}}{L_{Top}} \quad (13)$$

$$C_{Cell} = \frac{C_{NW}C_{Top}}{C_{Top}+C_{NW}} \quad (14)$$

where A is the cell cross-sectional area, L_{NW} the NW length, L_{Top} the thickness of the insulating layer on top of the NW as shown in **Figure 1**.

In our previous works, [27] we have demonstrated that the maximum average power is equal to:

$$P_{opt} = \frac{(V_{OC})^2}{2R_{opt}} \quad (15)$$

where V_{OC} is the root mean square (rms) value of the open-circuit voltage and R_{opt} is the optimum resistance of the unit cell:

$$R_{opt} = \frac{1}{C_{Cell}.\omega} \quad (16)$$

with C_{Cell} the capacitance of the unit cell which is given by the following expression as a function of the NWs capacitance C_{NW} and the top insulator capacitance C_{Top}:

$$C_{Cell} = \frac{C_{NW}C_{Top}}{C_{NW}+C_{Top}} \quad (17)$$

HyMeSoVING (Hybrid Method for Simulation of VING) will be used in order to evaluate the sensitivity of VING performance to the values of Young's modulus and dielectric permittivity of the filler, compared with the NWs volume fraction. The final objective is to provide guidelines on the best approach to optimize the VING device.

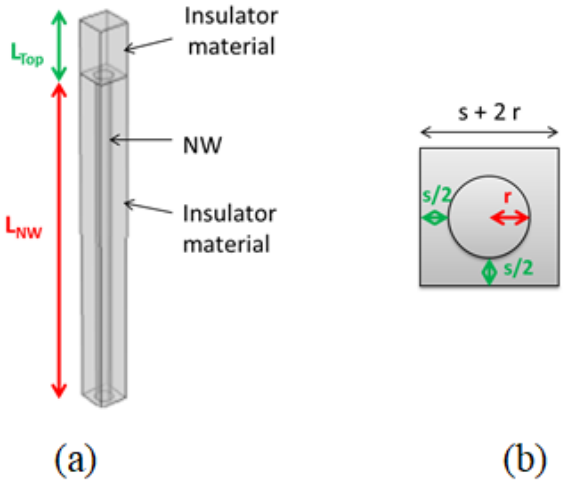

Figure 2: (a) Elementary cell including one ZnO nanowire surrounded by an insulating filler material; (b) Transversal cut of the elementary cell.

3. Results and discussions

3.1. Geometrical and physical properties of the unit cell

For the present study, and as in our previous works, [27] we consider ZnO NWs with a radius r of 50 nm and a length L_{NW} of 1.98 µm. The NWs are surrounded by a polymer matrix of Parylene C with a residual thickness L_{Top} of 300 nm on top of the NWs. The spacing s between neighbor NWs is set to 70 nm (**Figure 2.b**), corresponding to a NW volume fraction δ of 27%. Dielectric loss factor of Parylene C is set as isotropic one, with a value of 0.2%. [46] Electrodes are simulated as equipotential surfaces, which mean that a floating potential is assigned to the top electrode and ground to the bottom one. A mechanical boundary load is set on the top boundary at -5 N/cm², corresponding to usual experimental tests performed on the dedicated test bench.[16,17] The top electrode is implemented as a rigid connector in order to ensure the homogeneity of the applied load at the top surface of the cell. The mechanical boundary between the NWs and the polymer matrix is considered as ideal: thus, there is neither shear stress nor sliding movement between ZnO NW and the polymer matrix. An harmonic analysis is performed for an excitation frequency of 5 Hz because ambient sources are usually low, below 200 Hz [47] which is very far from the natural resonance frequency of the NWs (in the MHz range).[48]

The materials properties used for the following simulations are in the library of COMSOL Multiphysics:

• Stiffness tensor of ZnO:

$$c_{ij}^{E} = \begin{bmatrix} 2.09714 & 1.2114 & 1.05359 & 0 & 0 & 0 \\ 1.2114 & 2.09714 & 1.05359 & 0 & 0 & 0 \\ 1.05359 & 1.05359 & 2.11194 & 0 & 0 & 0 \\ 0 & 0 & 0 & 0.42373 & 0 & 0 \\ 0 & 0 & 0 & 0 & 0.42373 & 0 \\ 0 & 0 & 0 & 0 & 0 & 0.44248 \end{bmatrix} \times 10^{11}$$

• Coupling tensor of ZnO:

$$e_{ij} = \begin{bmatrix} 0 & 0 & 0 & 0 & -0.480508 & 0 \\ 0 & 0 & 0 & -0.480508 & 0 & 0 \\ -0.567005 & -0.567005 & 1.32044 & 0 & 0 & 0 \end{bmatrix}$$

• ZnO relative dielectric permittivity:

$$\epsilon_{ij}^{S} = \begin{bmatrix} 8.5446 & 0 & 0 \\ 0 & 8.5446 & 0 \\ 0 & 0 & 10.204 \end{bmatrix}$$

• ZnO dielectric losses: 1%

• Parylene C dielectric permittivity:

$$\epsilon_{ij}^{F} = \begin{bmatrix} 2.95 & 0 & 0 \\ 0 & 2.95 & 0 \\ 0 & 0 & 2.95 \end{bmatrix}$$

• Parylene C Young's Modulus: 2.8 GPa

• Parylene C Poisson's ratio: 0.3

Moreover, even if piezoelectric constants are well known for bulk materials, their values usually differ for MEMS (Micro-Electro-Mechanical Systems) and NEMS (Nano-Electro-Mechanical Systems). They depend on the material structure (thin or thick film, nanowire…) and manufacturing process (screen printing, Pulsed Laser Deposition, Vapor–Liquid–Solid deposition, hydrothermal synthesis). Moreover, at these scales, measuring directly or indirectly the piezoelectric constants is difficult, due to the substrate presence in the case of thin films [49] or inherent to the nanometer scale of nanowires.[8] However, Novak *et al.*[50] have determined experimentally the d_{33} coefficient and obtained a value of $6\ pC/N$. In our simulation, based on the used e_{ij} tensor, it is possible to deduce the corresponding value of d_{33} coefficient by using the following formula, which is valid under one-dimensional assumption: $d_{33} = e_{33}/c_{33}$, leading to $d_{33} = 5.6\ pC/N$ which is thus conform with literature.[50]

3.2. Strategy of optimization of the VING targeting the maximum average power

By both simulation and experimental results, it has been shown that the VING performances depend significantly on the NWs volume fraction δ.[5, 51] The present study aims at comparing the sensitivity of the VING performances (electric potential and average power) to 2 kinds of parameters: the NWs volume fraction and the filler material properties.
First, the effect of the NWs volume fraction δ is studied, considering Parylene C as the filler. **Figure 3** shows the open-circuit voltage and the average power as a function of δ.

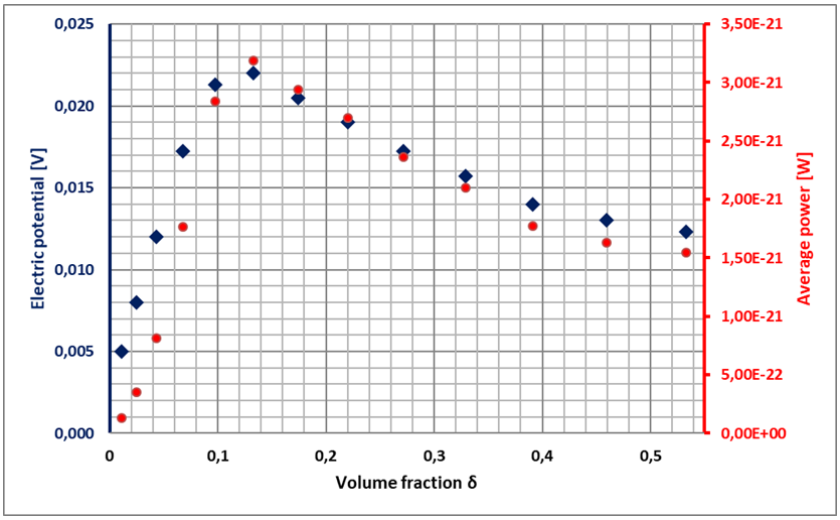

Figure 3: Open-circuit voltage and average power as a function of the volume fraction δ for a ZnO-Parylene C unit cell.

The maximum voltage (21 mV) is obtained for δ equal to 12.5% and the maximum power (3.21 zW) is obtained for δ equal to 13%. Thus, compared to the initial value (27%) of the volume fraction chosen in this theoretical study,[27] the δ value maximizing the electric potential improves the latter by 28%, and the δ value maximizing the average power improves the latter by 35%.
In order to compare the strategies of tuning the NWs density or optimizing the filler material, four types of materials were studied as the filler in the VING elementary cell: Parylene C, PMMA, PDMS and Al_2O_3. The values of both Young's modulus and permittivity of each material are presented in **Table 3**. Results of the four simulations performed using HyMeSoVING method are presented in **Table 3**. The geometrical and physical properties of the unit cell are unchanged, except the 2 above properties of the filler.

Table 3: Electrical characteristics of the VING deduced by HyMeSoVING method, as a function of the filler material

Filler material	**PDMS**	**Parylene C**	**PMMA**	**Al_2O_3**
Young's Modulus	750 kPa	2.8 GPa	3 GPa	400 GPa
Relative permittivity	2.75	2.95	3	5.7
Dielectric losses (%)	1 [53]	1 [45]	1.7 [52]	0.05 [54]
V_{OC} (mV)	82.02	17.25	15.99	0.27
C_{cell} (F)	4.83×10^{-19}	5.02×10^{-19}	5.07×10^{-19}	7.5×10^{-19}

(eq. 14)				
R_{opt} (Ω) (eq. 16)	6.53×10^{16}	6.29×10^{16}	6.23×10^{16}	4.22×10^{16}
P_{opt} (W) (eq. 15)	5.15×10^{-20}	2.37×10^{-21}	2.05×10^{-21}	9.17×10^{-25}

Simulation results show that the single cell VING containing PDMS, which has the lowest Young's modulus (750 kPa) and permittivity (2.75), generates the highest voltage (4.7 times the one generated with Parylene C) and average power (22 times the one obtained with Parylene C).

Since that above results showed that the PDMS, which has the lowest Young's modulus and permittivity, generates the highest voltage and power, HyMeSoVING method is used in order to evaluate the effect of the filler's Young's modulus and the permittivity on the VING characteristics.

For the first study, the filler's permittivity is fixed to 2.95 and only the Young's modulus is varied from 500 kPa to 400 GPa. This range is chosen since the most used filler materials have a Young's Modulus of some GPa.[5, 18, 52, 53] Results are presented in **Figure 4**.

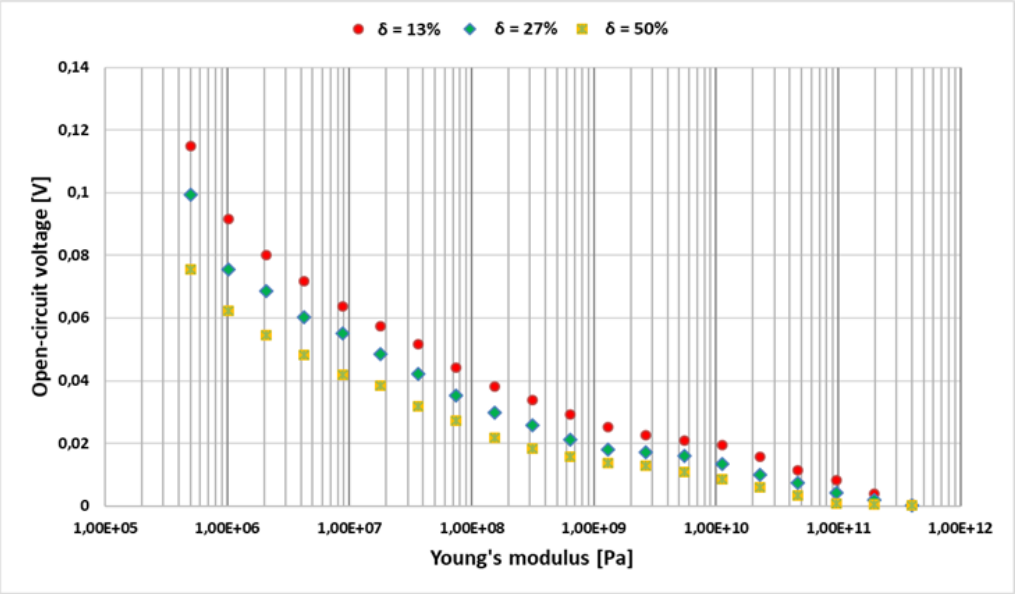

(a)

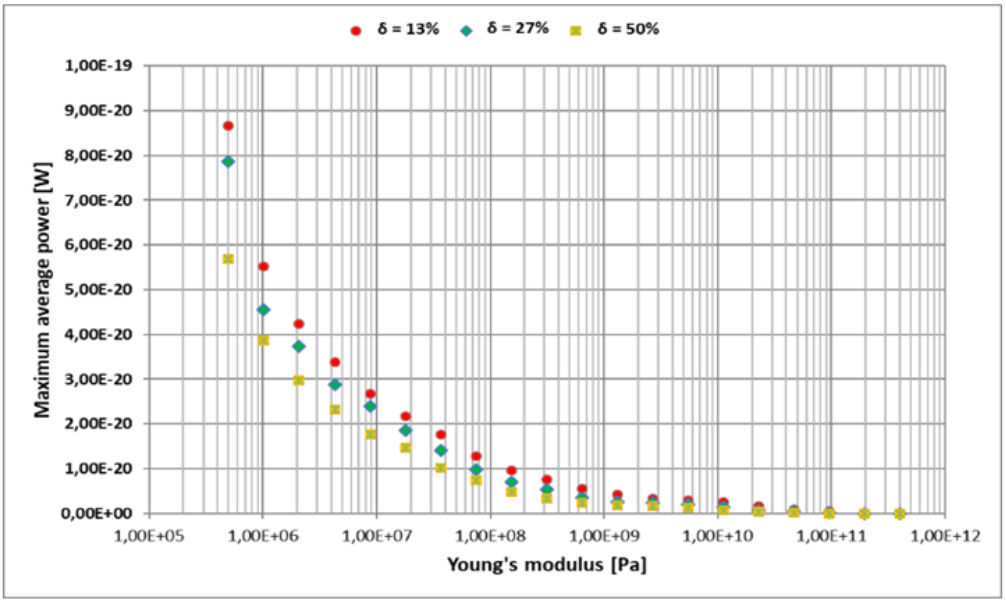

(b)

Figure 4: (a) Open-circuit voltage and (b) Maximum average power as a function of the filler Young's modulus for several ZnO volume fractions δ.

Figure 4 shows that the higher the Young's modulus, the lower the generated voltage and the average power of the elementary cell. In fact, for a volume fraction of 27%, the Parylene C Young's modulus (2.8 GPa) gives an open-circuit voltage 30% higher and an average power 66% higher than a material with a 10 GPa Young's modulus. We can also observe that for a volume fraction of 13% the generated voltage and the average power are higher than the other studied volume fractions. This is because this value is close to the optimum NWs density values giving the maximum voltage (optimum density 12.5%) and average power (optimum density 13%).

The second set of studies consists in fixing the filler Young's modulus to 2.8 GPa and varying its relative dielectric permittivity from 1 to 7, a range corresponding to the most usual filler materials.[5, 18, 52, 53] Results are presented **Figure 5**.

Figure 5 shows that the higher the permittivity, the lower the generated voltage and the average power of the elementary cell. In fact, for a volume fraction of 27%, the Parylene C permittivity (2.95) gives an open-circuit voltage 70% higher and an average power 64% higher than a material with a permittivity equal to 7.

Based on all the above studies, it appears that choosing an optimal filler material with low Young's modulus and permittivity is more powerful than changing the NWs fraction.

Of course, the deposition methods of the different fillers are not the same, and the thickness of the residual layer on top of the NW is often different, which influences also the efficiency of the VING. In reference 18, the top layer is 7 µm thick for PDMS deposited by spin coating, in reference 54 the top layer of spin-coated PMMA is around 1 µm, whereas in reference 16 this layer is 200 nm thick for Parylene C deposited by Chemical Vapor Deposition (CVD). A thick layer atop the NWs is expected to lower the VING performance.[15] Changing the filler material while maintaining a thin residual layer atop the NWs is not straightforward, as it strongly depends on the process used to deposit the filler material, and on the capacity of the filler to infiltrate the NWs array. This aspect makes a comparison between different prototypes very difficult, especially since experimental testing conditions usually vary from one study to another.

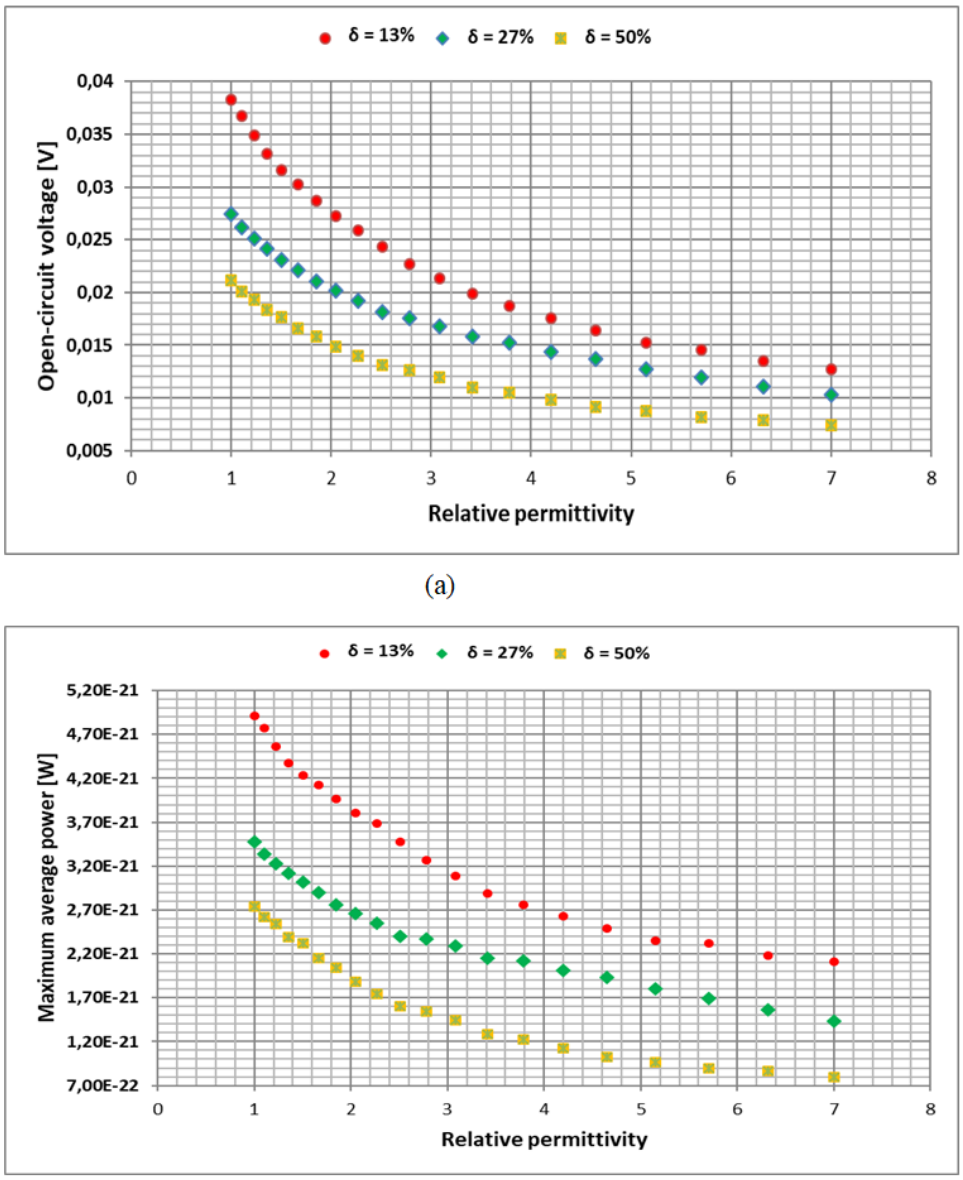

Figure 5: (a) Open-circuit voltage and (b) Maximum average power as a function of the filler relative permittivity for several ZnO volume fractions δ.

Nevertheless, the present study demonstrates that, for a given configuration of VING (with a particular set of geometrical dimensions), the sensitivity of the VING performances on various parameters (here the NWs volume fraction and the filler mechanical and dielectric properties) is worth being quantified before performing an optimization of the various parts of the VING structure.

4. Conclusion

In this paper, the effect of electrical and mechanical properties (Young's modulus and dielectric permittivity) of the filler in a VING elementary cell was studied based on a previous work.[27] Results show that a filler material with low Young's modulus and dielectric permittivity gives higher values of generated voltage and power. Among 4

materials usually used in VING devices, PDMS which has the lower Young's modulus (750 kPa) and permittivity (2.75) is expected to provide the highest voltage (4.7 times than the one obtained with Parylene C) and average power (22 times higher than with Parylene C) generated by the single cell. Moreover, optimizing the filler appears to have much more influence on the VING output performance than optimizing the NW's volume fraction. In further works, HyMeSoVING method will be used in order to determine which properties should have the optimal piezoelectric material in order to further improve the VING performance. The effect of the irregular length, shape and alignment of the NWs within the full NWs array will also be investigated.

Acknowledgements

This work was supported by EnSO project. EnSO has been accepted for funding within the Electronic Components and Systems For European Leadership Joint Undertaking in collaboration with the European Union's H2020 Framework Programme (H2020/2014-2020) and National Authorities [Grant agreement No. 692482].

References

[1] L. Jin, B. Zhang, L. Zhang and W. Yang, *Nano Energy* **2019**, *66*, 104086, DOI: 10.1016/j.nanoen.2019.104086.
[2] Y. Chang, J. Zuo, H. Zhang and X. Duan, *Nanotechnology and Precision Engineering* **2020**, *3*, 43.
[3] S. S. Indira , C. A. Vaithilingam , K. S. Prakash Oruganti, F. Mohd and S. Rahman, *Nanomaterials* **2019**, *9*, 773.
[4] M. Choi, G. Murillo, S. Hwang, J. W. Kim, J. H. Jung, C.-Y. Chen and M. Lee, *Nano Energy* **2017**, *33*, 462.
[5] R. Hinchet , S. Lee, G. Ardila, L. Montès, M. Mouis and Z. L. Wang, *Advanced Functional Materials* **2013**, *24*, 971.
[6] N. Gogneau, N. Jamond, P. Chrétien, F. Houzé, E. Lefeuvre and M. Tchernycheva, *Semiconductor Science and Technology* **2016**, *31*, 103002.
[7] X. Li, M. Sun, X. Wei, C. Shan and Q. Chen, *Nanomaterials* **2018**, *8*, 188.
[8] Z. L. Wang and J. Song, *Science* **2006**, *312*, 242.
[9] R. Yang, Y. Qin, L. Dai and Z. L. Wang, *Nature Nanotechnology* **2009**, *4*, 34.
[10] X. Chen, S. Xu, N. Yao and Y. Shi, *Nano Letters* **2010**, *10*, 2133.
[11] S. Xu, Y. Qin, C. Xu, Y. Wei, R. Yang and Z. L. Wang, *Nature Nanotechnology* **2010**, *5*, 366.
[12] Y. Qin, X. Wang and Z. L. Wang, *Nature* **2008**, *451*, 809.
[13] M. Lee, C.-Y. Chen, S. Wang, N. C. Cha, Y. J. Park, J. M. Kim, L.-J. Chou and Z. L. Wang, *Advanced Materials* **2012**, *24*, 1759.
[14] X. Wang, J. Song, J. Liu and Z. L. Wang, *Science* **2007**, *316*, 102.
[15] R. Hinchet, S. Lee, G. Ardila, L. Montès, M. Mouis and Z. L. Wang, *Journal of Energy and Power Engineering* **2013**, *7*, 1816.
[16] A. Dahiya, F. Morini, S. Boubenia, K. Nadaud, D. Alquier and G. Poulin-Vittrant, *Advanced Materials Technologies* **2017**, *3*, 1700249.
[17] G. Poulin-Vittrant, C. Oshman, C. Opoku, A. Dahiya, N. Camara, D. Alquier, L. P. Tran Huu Hue and M. Lethiecq, *Physics Procedia* **2015**, *70*, 909.
[18] C. Opoku, A. Dahiya, F. Cayrel, G. Poulin-Vittrant, D. Alquier and N. Camara, *Royal Society of Chemistry Advances* **2015**, *5*, 69925.

[19] C.-T. Huang, J. Song, W.-F. Lee, Y. Ding, Z. Gao, Y. Hao, L.-J. Chen and Z. L. Wang, *Journal of the American Chemical Society* **2010**, *132*,4766.
[20] C.-Y. Chen, G. Zhu, Y. Hu, J.-W. Yu, J. Song, K.-Y. Cheng, L.-H. Peng, L.-J. Chou and Z. L. Wang, *ACS Nano* **2012**, *6*, 5687.
[21] L. Gu, N. Cui, L. Cheng, Q. Xu, S. Bai, M. Yuan, W. Wu, J. Liu, Y. Zhao, F. Ma, Y. Qin and Z. L. Wang, *Nano Letters* **2013**, *13*, 91.
[22] Y. Qi, J. Kim, T. D. Nguyen, B. Lisko, P. K. Purohit and M. McAlpine, *Nano Letters* **2011**, *11*, 1331.
[23] K.-I. Park, S. Xu, Y. Liu, G.-T. Hwang, S.-J. L. Kang, Z. L. Wang and K. J. Lee, *Nano Letters*, 2010, **10**, 4939.
[24] Z.-H. Lin, Y. Yang, J. M. Wu, Y. Liu, F. Zhang and Z. L. Wang, *The Journal of Physical Chemistry Letters* **2012**, *3*, 3599.
[25] J. H. Jung, M. Lee, J.-I. Hong, Y. Ding, C.-Y. Chen, L.-J. Chou and Z. L. Wang, *ACS Nano* **2011**, *5*, 10041.
[26] C. Chang, V. H. Tran, J. Wang, Y.-K. Fuh and L. Lin, *Nano Letters* **2010**, *10*, 726.
[27] N. Doumit and G. Poulin-Vittrant, *Advanced Theory and Simulations* **2018**, *1*, 1800033.
[28] D. Armani, C. Liu and N. Aluru, in Technical Digest. *IEEE International MEMS 99 Conference, Twelfth IEEE International Conference on Micro Electro Mechanical Systems*, Orlando, USA, **1999**.
[29] C. Hassler, R. P. Von Metzen, P. Ruther and T. Stieglitz, *Journal of Biomedical Materials Research* **2010**, *93B*, 266.
[30] A. Boger, K. Wheeler, A. Montalli and E. Gruskin, *Journal of Biomedical materials Research – Part B – Applied biomaterials* **2010**, *93B*, 266.
[31] M. A. El-Shahawy, *Polymer testing* **1999**, *18*, 389.
[32] J. F. Schackelford and W. Alexander, Materials Science and Engineering Handbook, *Boa Raton : CRC Press* **2001**.
[33] A. Kachroudi, S. Basrour, L. Rufer, A. Sylvestre and F. Jomni, *Smart Materials and Structures* **2015**, *24*, 125013.
[34] A. Kahouli, A. Sylvestre, L. Ortega, F. Jomni, B. Yangui, M. Maillard, B. Berge, J. C. Robert and J. Legrand, *Applied Physics Letters* **2009**, *94*, 152901.
[35] P. R. Sreehitha, B. Durga and M. Balachandran, *Materials Today: Proceedings* **2020**, *24*, 772.
[36] P. Bandyopadhyay, M. Dwivedi, H. Krishnaswamy and P. Ghosh, *Polymer* **2020**, *191*, 122274.
[37] R. Tao, R. Hinchet, G. Ardila and M. Mouis, *Journal of Physics: Conference Series* **2013**, *476*, 012006.
[38] L.-Y. Chen and G. W. Hunter, in *2004 MRS Fall Meeting* **2004**, Boston.
[39] W. Martienssen and H. Warlimont, *Springer Handbookof Condensed Matter and Materials Data*, Germany, *Springer*, **2005**
[40] A. Yu, H. Li, H. Tang, T. Liu, P. Jiang and Z. L. Wang, *Physica Status Solidi (RRL)* **2011**, *5*, 162.
[41] L. Lu, N. Jamond, P. Chrétien, F. Houzé, F. Travers, J. Harmand, F. Glas, F. Julien, N. Gogneau and M. Tchernycheva*, Journal of Physics: Conference Series* **2016**, *773*, 012010.
[42] H. Sun, H. Tian, Y. Yang, Y.-C. Zhang, X. Liu, S. Ma, H.-M. Zhao and T.-L. Ren, *Nanoscale* **2013**, *5*, 6117.
[43] S. Kannan, M. Parmar, R. Tao, G. Ardila and M. Mouis, *Journal of Physics: Conference Series* **2016**, *773*, 012071.

[44] W. A. Smith and B. A. Auld, *IEEE Transactions on Ultrasonics, Ferroelectrics, and Frequency Control* **1991**, *38*, 40.
[45] N. S. Ottosen and M. Ristinmaa, *The Mechanics of Constitutive Modeling*, Elsevier, Sweeden **2005**.
[46] C. Kärnfelt, C. Tegnander, J. Rudnicki, J. P. Starski and A. Emrich, *IEEE Transactions on Microwave Theory and Techniques* **2006**, *54*, 3417.
[47] S. Roundy, P. K. Wright and J. Rabaey, *Computer Communications*, **2003**, *26*, 1131.
[48] S. Timoshenko, D. H. Young and W. Weaver, *Vibration Problems in Engineering,* Wiley, New York **1974**.
[49] A. Barzegar, D. Damjanovic, N. Ledermann and P. Muralt, *Journal of Applied Physics* **2003**, *93*, 4756.
[50] N. Novak, P. Keil, F. F. Schader, A. Martin, K. G. Webber and J. Rodel, *Acta Materialia* **2019**, *162*, 277.
[51] D. Yang, Y. Qiu, Q. Jiang, Z. Guo, W. Song, J. Xu, Y. Zong, Q. Feng and X. Sun, *Applied Physics Letters* **2017**, *110*, 63901.
[52] Y. Hu, L. Lin, Y. Zhang and Z. L. Wang, *Advanced Materials* **2012**, *24*, 110.
[53] S. Xu, C. Xu, Y. Liu, Y. Hu, R. Yang, Q. Yang, J.-H. Ryou, H. J. Kim, Z. Lochner, S. Choi, R. Dupuis and Z. L. Wang, *Advanced Materials* **2010**, *42*, 4749.
[54] G. Zhu, A. C. Wang, Y. Liu, Y. Zhou and Z. L. Wang, *Nano Letters* **2012**, *12*, 3086.